



## Article

DNA-assisted rational design of BaF<sub>2</sub> linear and erythrocyte-shaped nanocrystals☆

Xinmei Zhao, Huanhuan You, Faming Gao \*

Key Laboratory of Applied Chemistry, Department of Applied Chemistry, Yanshan University, Qinhuangdao 066004, China

## ARTICLE INFO

## Article history:

Received 25 October 2017

Received in revised form 20 December 2017

Accepted 17 January 2018

Available online 10 February 2018

## Keywords:

DNA-assistance

BaF<sub>2</sub>

Morphology

Linear arranged nanoparticles

Erythrocyte-shaped structure

## ABSTRACT

The synthesis of inorganic materials with special morphologies with the assistance of biological molecules is a potential development in the field of controllable growth and assembly of nanomaterials. In this paper, BaF<sub>2</sub> nanocrystals in patterns of well-defined linear and erythrocyte-shaped structure were synthesized with the assistance of *Escherichia coli* DNA. Morphology and the arrangement of BaF<sub>2</sub> particles on DNA were controllable by altering the reaction condition. Square nanoparticles arranged in linear chains were gained with the assistance of normal DNA; while, erythrocyte-shaped BaF<sub>2</sub> nanospheres were synthesized with the assistance of denatured DNA. Besides, the influences of solvent, reaction temperature, concentration of reactants and the heating time on the morphology of the BaF<sub>2</sub> particles were studied.

© 2017 The Chemical Industry and Engineering Society of China, and Chemical Industry Press. All rights reserved.

## 1. Introduction

As an acknowledged ideal fast scintillator, Barium fluoride is one of the dielectric fluorides (CaF<sub>2</sub>, SrF<sub>2</sub>, and BaF<sub>2</sub>) that have a wide range of potential applications in microelectronic and optoelectronic devices, such as wide-gap insulating overlayers, gate dielectrics, insulators and buffer layers in semiconductor-on-insulator structures, and more advanced three dimensional structure devices [1,2]. So far, hydrothermal method, chemical surface modification, precipitation method, and spark plasma sintering were mostly used to synthesize BaF<sub>2</sub> [3–6]. While, the disadvantages of methods mentioned above are obvious, for example, higher temperature and sophisticated devices are needed, *et al.* If a new facile synthesis method can be developed, it may be popular.

With the intercrossing and infiltrating of Biology and Nano-chemistry, morphology-controlled synthesis of inorganic nanostructure has drawn significant interests [7–12]. With the advantages of simple installation, facile reaction condition and morphologies easy to control, it's a potential development in the field of controllable synthesis of micro/nano materials. Besides, biological molecules are diverse, renewable and eco-friendly [13]. Among these ideal biotemplates, Deoxyribonucleic acid (DNA) was one of the earliest used bio-templates [14–17] and it's also a potentially ideal template to dictate the precise positioning of molecules into any deliberately designed structure due to its remarkable molecular recognition properties and structural features [18–21]. Kinds of noble

metallic nanowires [22–25] and semiconductor nanowires [26,27] have been prepared using DNA as the bio-template, while BaF<sub>2</sub> nanostructure synthesized with the assistance of DNA was rarely reported [28].

In our study, we report a facile method for efficiently attaching BaF<sub>2</sub> nanocrystals with well-defined linear and erythrocyte-shaped structure to DNA skeleton respectively. Morphologies and the arrange manner of BaF<sub>2</sub> particles on DNA depend on the reaction condition. Possible mechanism of different morphologies associated with the DNA's conformational changes is discussed briefly in the end.

## 2. Experimental

## 2.1. Chemicals

All reagents used here were analytical reagent and used as received without further purification. Barium nitrate and ammonium fluoride were purchased from Tianjin Guangfu fine chemical industry research institution. Absolute ethanol, sodium dodecyl sulfate (SDS) and DMSO were purchased from Tianjin Kermel Chemical Reagent Co., Ltd.. Aqueous stock solution of the *Escherichia coli* (*E. coli*) B genomic DNA was freshly prepared. Doubly distilled water was used in this work.

## 2.2. Synthetic protocol

2.2.1. Extraction of *E. coli* B genomic DNA

To get the biotemplates, a stock solution of *E. coli* B genomic DNA was firstly prepared. *E. coli* B cells were cultured overnight in 50 ml of LB medium. Then, the cells were collected by centrifugation and resuspended in TE buffer [10 mmol·L<sup>-1</sup> Tris (pH 8.0), 1 mmol·L<sup>-1</sup> EDTA

☆ Supported by the National Natural Science Foundation of China (Nos. 21371149, 21671168) and the Natural Science Foundation of Hebei Province (Nos. B2016203498, GCC2014009).

\* Corresponding author.

E-mail address: [fmgao@ysu.edu.cn](mailto:fmgao@ysu.edu.cn) (F. Gao).

(pH 8.0)]. Then, 10% SDS and  $10 \text{ mg} \cdot \text{ml}^{-1}$  proteinase K were added to adequately disassemble the cells in a  $50^\circ\text{C}$  water bath for 30 min. The mixture was extracted with equal volume phenol:chloroform:isoamyl alcohol (25:24:1) and centrifuged at  $5000 \text{ r} \cdot \text{min}^{-1}$  for 10 min. The aqueous supernatant was transferred to a new tube. The extraction process can be repeated if it's necessary. Then 2-fold volume absolute ethanol was added to the supernatant. Then it was placed under room temperature for 30 min and centrifuged at  $12000 \text{ r} \cdot \text{min}^{-1}$  for 10 min. The DNA precipitate was washed with 70% ethanol more than twice. Finally DNA was dissolved in deionized water. The nucleic acid and protein analysis was used to check the purity of DNA.

### 2.2.2. Preparation of $\text{BaF}_2$ nanocrystals with DNA assisted

In this work, we used DNA with high purity ( $\text{OD} \approx 1.8$ ) as biotemplate to design and assemble a series of  $\text{BaF}_2$  nanocrystals with different sizes and morphologies. The basic protocol for the synthesis of  $\text{BaF}_2$  nanocrystal is described as follows: firstly, aqueous solution of  $\text{Ba}(\text{NO}_3)_2$  ( $50 \mu\text{l}$ ,  $0.1 \text{ mol} \cdot \text{L}^{-1}$ ) was added to the solution of *E. coli B* genomic DNA ( $1.2 \mu\text{g} \cdot \mu\text{l}^{-1}$ ) as prepared above and the solution was mixed thoroughly and incubated for 5 h at  $6^\circ\text{C}$ ; secondly, aqueous solution of  $\text{NH}_4\text{F}$  ( $50 \mu\text{l}$ ,  $0.2 \text{ mol} \cdot \text{L}^{-1}$ ) was dropped. The solution was mixed thoroughly again and incubated for another 3 h at  $6^\circ\text{C}$ ; In the end, the mixture was heated and kept at  $40^\circ\text{C}$  for 2 h. All the samples as prepared were stored at  $4^\circ\text{C}$  for further study.

### 2.3. Characterization

The morphologies of the samples were observed by transmission electron microscope (TEM). A droplet ( $20 \mu\text{l}$ ) of the samples was dropped onto a 300-mesh carbon-coated copper grid and then air-dried before TEM observation. It was carried out on a JEM-2010 electron microscope instrument operated at an accelerating voltage of 200 kV. The chemical composition and crystal structure were established by energy-dispersive X-ray spectroscopy (EDXS) and selected-area electron diffraction (SAED) respectively.

## 3. Results and Discussion

The *E. coli B* Genomic DNA is a circular double-stranded DNA (dsDNA) with 1.3 mm in length and it contains 4.6 Mb base pairs. DNA's remarkable molecular recognition properties and structural features make it one of the most promising templates to pattern materials with nanoscale precision [29]. DNA strands can offer a variety of binding sites for metal ions such as  $\text{Ba}^{2+}$ .

Fig. 1 shows the typical features of DNA-assisted  $\text{BaF}_2$  nanocrystals. Samples were synthesized with equal volume ( $50 \mu\text{l}$ ) of  $0.1 \text{ mol} \cdot \text{L}^{-1}$   $\text{Ba}(\text{NO}_3)_2$  and  $0.2 \text{ mol} \cdot \text{L}^{-1}$   $\text{NH}_4\text{F}$  solutions and incubated at  $40^\circ\text{C}$ . The heating time were 0.5 h (S1, shown in Fig. 1a), 1 h (S2, shown in Fig. 1c), 2 h (S3, shown in Fig. 1d) respectively. All samples were directly characterized by TEM without any negative staining. As shown in Fig. 1a, irregular ring structures with several microns in size were observed in the product of S1 heated for 0.5 h, and Fig. 1b shows the higher magnified TEM image of S1. With the extension of heating time, the ring structures of S2 heated for 1 h became approximate circles with a diameter of  $2.5 \mu\text{m}$  around (as shown in Fig. 1c). However, the ring structures blasted to linear chains gradually when it was heated for 2 h (as shown in Fig. 1d).

The formation mechanism of the ring structures can be explained vividly by Fig. 2. And similar ring structure was obtained in our previous report [30]. In order to investigate which kind of bases played a major role on the formation of nanocrystal, Li used Oligo(dT), Oligo(dA), Oligo(dG) and Oligo(dC) as the template respectively. And it revealed that the phosphate and possibly the amino moiety binding

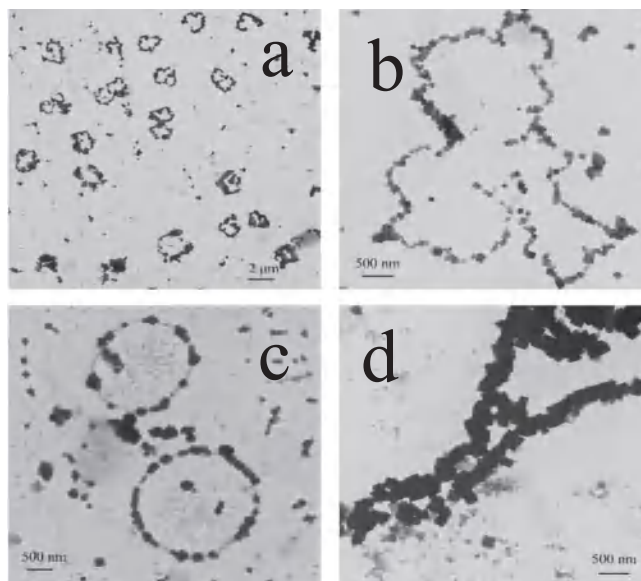


Fig. 1. TEM images of DNA-assisted  $\text{BaF}_2$  nanocrystals incubated at  $40^\circ\text{C}$  with different heating time respectively: (a) 0.5 h, (c) 2 h. (b) shows the higher magnified TEM image of S1.

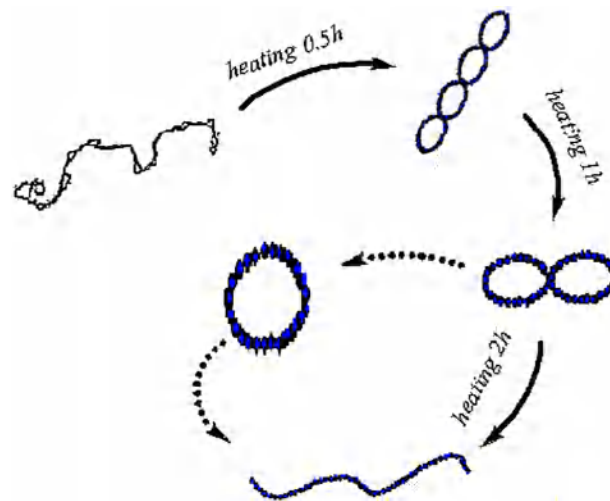
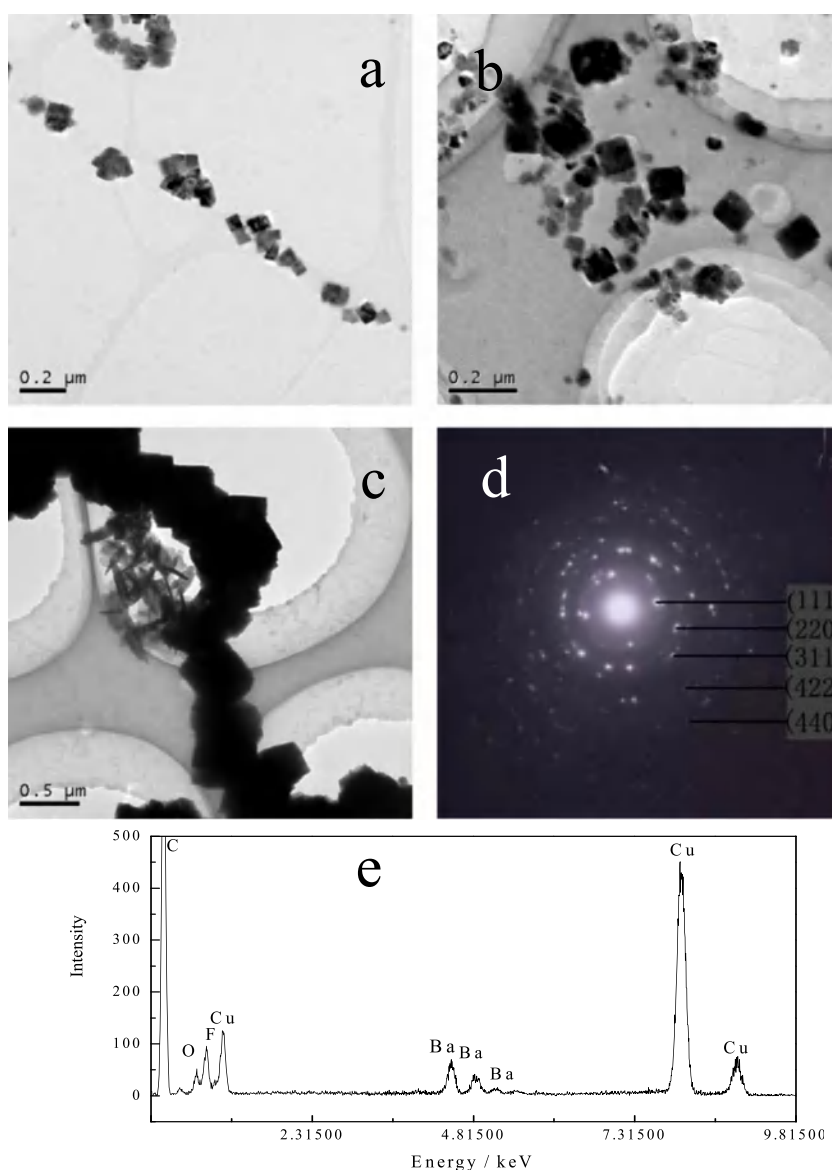


Fig. 2. The formation mechanism of the ring structures.

site on adenine are the favorable targets to feed nanoparticle growth [31].

To investigate the metallization process further, we studied the effect of reagent concentration, taking the linear-chain structure for example. Samples of S4, S5 and S6 were prepared with the concentration ratios of  $\text{Ba}(\text{NO}_3)_2/\text{NH}_4\text{F}$  ( $0.1 \text{ mol} \cdot \text{L}^{-1}:0.2 \text{ mol} \cdot \text{L}^{-1}$ ,  $0.2 \text{ mol} \cdot \text{L}^{-1}:0.4 \text{ mol} \cdot \text{L}^{-1}$  and  $0.3 \text{ mol} \cdot \text{L}^{-1}:0.6 \text{ mol} \cdot \text{L}^{-1}$ , respectively).  $20 \mu\text{l}$   $\text{Ba}(\text{NO}_3)_2$  and  $\text{NH}_4\text{F}$  solution were added successively. The morphologies of the  $\text{BaF}_2$  nanocrystals aggregated on DNA were revealed by TEM images, as shown in Fig. 3.  $\text{BaF}_2$  nanoparticles attached to the strand of DNA were arranged in linear structure discontinuously. The average particle size (equivalent diameter) of S4 in Fig. 3a was 58 nm (20 particles were used to calculate the average values and the standard deviation was 21 nm). The average particle size of S5 was 102 nm (20 particles were calculated and the standard deviation was 11 nm), and the dispersion of the particles were uneven obviously, compared to S6 (equivalent diameter was about 400 nm). It demonstrated that the



**Fig. 3.** (a–c) TEM images of  $\text{BaF}_2$  nanocrystals aggregated on DNA linear chains with different concentration ratios of  $\text{Ba}(\text{NO}_3)_2/\text{NH}_4\text{F}$ . (a) S4  $0.1 \text{ mol}\cdot\text{L}^{-1}$ :  $0.2 \text{ mol}\cdot\text{L}^{-1}$ , (b) S5  $0.2 \text{ mol}\cdot\text{L}^{-1}$ :  $0.4 \text{ mol}\cdot\text{L}^{-1}$  and (c) S6  $0.3 \text{ mol}\cdot\text{L}^{-1}$ :  $0.6 \text{ mol}\cdot\text{L}^{-1}$ , respectively. (d) SAED pattern taken on the  $\text{BaF}_2$  nanoparticle linear chains shown in (a). (e) EDXS of the DNA-assisted  $\text{BaF}_2$  nanoparticles.

size of  $\text{BaF}_2$  nanoparticles could be tuned by altering the amount of Ba (II).

The concentration of DNA solution was closed for the samples, while excess of Ba(II) made the square nanoparticles bigger and continuously bind to the strand of DNA (shown in Fig. 3c). Fig. 3d shows the selected area electron diffraction (SAED) pattern recorded from  $\text{BaF}_2$  nanocrystal of S4. Through calculating, we found that diffraction rings corresponded to (111), (220), (311), (422) and (440) planes of cube structure of  $\text{BaF}_2$  respectively. It proved that  $\text{BaF}_2$  was well crystallized. Fig. 3e shows the patterns of EDXS. Peaks for the elements of Ba, F, O, C and Cu were observed. Cu and C peaks were due to the carbon-coated copper grid and O peak may arise from DNA. It's confirmed by SEAD and EDXS that we successfully synthesized cubic  $\text{BaF}_2$  nanocrystals with the assistance of DNA.

We also studied the solvent influence on the morphologies and size of  $\text{BaF}_2$  nanoparticles aggregated on DNA. Sample S7 was prepared using the mixture of water and ethanol (1:2) as solvent and reacted under the same conditions with S4. Then samples were directly detected under TEM and the images gained were shown in Fig. 4.

Insets of Fig. 4 (a) and (b) are higher magnification images of sample S4 and S7. By contrasting, we found square nanoparticles in S4 and nanospheres in S7 (with 74 nm in diameter, 20 particles were used to calculate the average values and the standard deviation was 23 nm). We propose that: when using pure water as solvent, there is maybe an obvious preferential growth phenomenon along some crystal faces, so crystals grow faster in these directions, and slower in the others, thus making it easier to form square nanoparticles. Meanwhile, with the adding of ethanol, the preferential growth of the particles is gradually weakened, eventually making the growth speeds along different crystal faces closed, thus making it easier to form nanospheres.

DsDNA molecule is stabilized by base stacking and the interaction can be disturbed relatively easily by thermal fluctuations [32]. DNA has various conformational transitions via its double-helix twisting or folding. Double strands even can be separated into single lines when it's heated to  $80^\circ\text{C}$  (denaturation temperature), creating nano pair-linear arrays. Herein, we also investigated a simple method for the preparation of different morphologies of  $\text{BaF}_2$

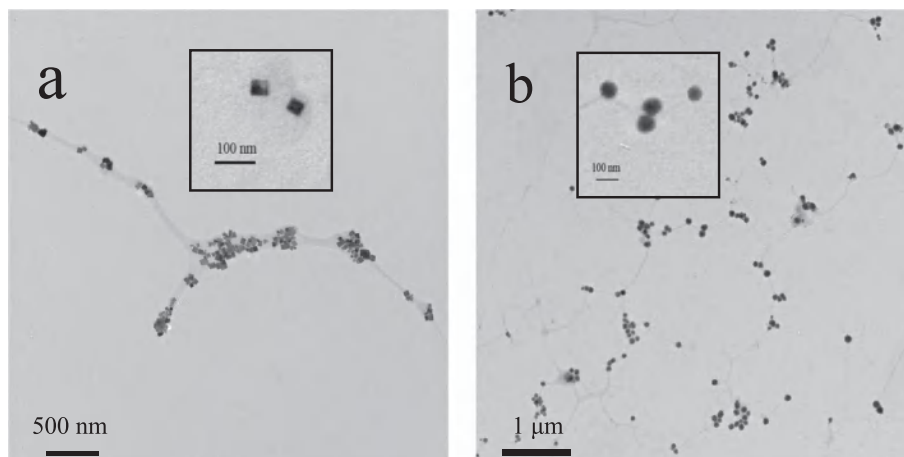


**Fig. 4.** Effect of solvents on product's morphologies, (a) S4: water as the solvent; (b) S7: mixture of water and ethanol (1:2) as the solvent. Inset of (a) show the arresting difference of BaF<sub>2</sub> nanocrystals taken on a higher magnification.

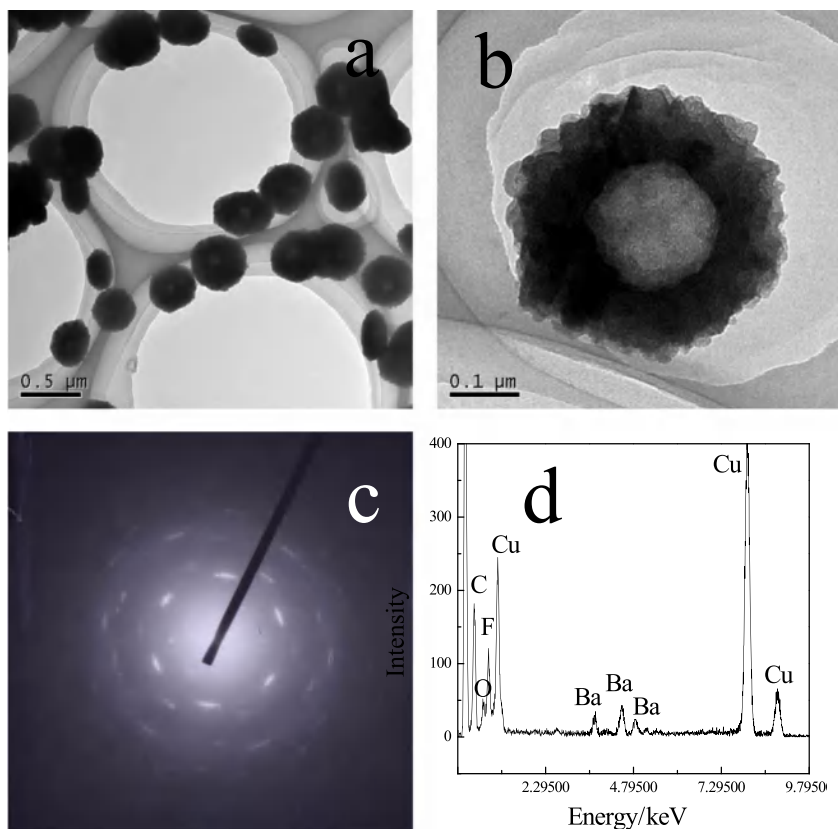
nanocrystals using denatured DNA (heated to 90 °C), as shown in Fig. 5. S8 was synthesized in the mixed solvent of ethanol and water (2:1). It proves that DNA's conformational change has a dramatic effect on the final products, leading to the formation of erythrocyte-shaped BaF<sub>2</sub> nanospheres. It was a totally different and novel morphology, unlike the BaWO<sub>4</sub> nano pair-linear arrays reported by Li *et al.*

Fig. 5a shows the monodisperse, size-uniformed and erythrocyte-shaped BaF<sub>2</sub> nanospheres. And Fig. 5b shows orthograph of the erythrocyte-shaped nanospheres observed under higher magnification. These erythrocyte-shaped nanospheres were about 400 nm in outer diameter with a hollow center. Moreover, the patterns of EDXS shown in Fig. 5c also indicated that we synthesized erythrocyte-shaped BaF<sub>2</sub> nanocrystals assisted by DNA successfully.

The mechanism of DNA assisted synthesis of BaF<sub>2</sub> is showed in Fig. 6 as follows. When Ba<sup>2+</sup> was added to DNA solution, it attached to DNA skeleton by electrostatic force and combined with phosphate groups on DNA. F<sup>-</sup> reacted with DNA-Ba<sup>2+</sup> compound and crystal nucleus of BaF<sub>2</sub> was formed, then square or spherical particles were fabricated along DNA chain with different size. The mechanism of the formation of the erythrocyte-shaped nanospheres was not so clear and more study will be done in our further work.

#### 4. Conclusions

Assisted by normal *E. coli B* circular dsDNA, we present an effective and efficient method for preparation of BaF<sub>2</sub> square nanocrystals



**Fig. 5.** TEM images of erythrocyte-shaped BaF<sub>2</sub> nanospheres prepared with denatured DNA treated at 90 °C. (b) A higher magnified TEM image of S8. (c) SAED pattern taken on the BaF<sub>2</sub> nanospheres shown in (a). (d) EDXS of the DNA-assisted BaF<sub>2</sub> nanospheres.

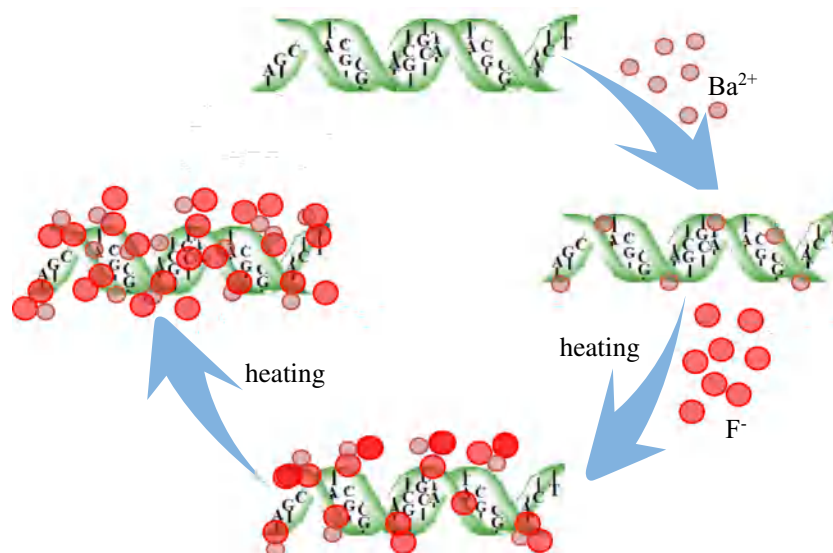


Fig. 6. Schematic diagram of DNA-assisted synthesis of BaF<sub>2</sub>.

arranged in irregular rings, circles to linear chains. These morphology differences are affected by conformational changes of the dsDNA super-helix, which can be disturbed relatively easily by thermal fluctuation. Thus, we can easily get various nano-patterns by regulating the heating time and DNA's conformation. An interesting result shows that mixed solvent of ethanol and water can obviously make the BaF<sub>2</sub> square nanocrystals become round. Based on this, we rationally designed one more kind of amazing nano-patterns, erythrocyte-shaped BaF<sub>2</sub> nanospheres, by using the denatured DNA.

Different morphologies of BaF<sub>2</sub> with the assistant of DNA templates were synthesized in our study, and even the linear-arrangement nanocrystals and erythrocyte-shaped nanocrystals of BaF<sub>2</sub> were synthesized for the first time. We expect that erythrocyte-shaped BaF<sub>2</sub> crystals, as a new morphology, may have the potential application in the future. So erythrocyte-shaped nanocrystals with uniform size, morphologies, good optical and mechanical properties is being studied in our present work. It's significant to the synthesis of BaF<sub>2</sub> with ideal application performance.

## References

- [1] G.H. De, W.P. Qin, J.S. Zhang, J.S. Zhang, Y. Wang, C.Y. Cao, Y. Cui, Synthesis and photoluminescence of single crystals europium ion-doped BaF<sub>2</sub> cubic nanorods, *J. Solid State Chem.* 179 (3) (2006) 955–958.
- [2] M.H. Cao, C.W. Hu, E.B. Wang, The first fluoride one-dimensional nanostructures: Microemulsion-mediated hydrothermal synthesis of BaF<sub>2</sub> whiskers, *J. Am. Chem. Soc.* 125 (37) (2003) 11196–11197.
- [3] J.M. Luo, S. Sahi, M. Groza, Z.Q. Wang, L. Ma, W. Chen, A. Burger, R. Kenarangui, T.K. Sham, F.A. Selim, Luminescence and scintillation properties of BaF<sub>2</sub>-Ce transparent ceramic, *Opt. Mater.* 58 (2016) 353–356.
- [4] T.M. Demkiv, O.O. Halyatkin, V.V. Vistovskyy, A.V. Gektin, A.S. Voloshinovsky, Luminescent and kinetic properties of the polystyrene composites based on BaF<sub>2</sub> nanoparticles, *Nucl. Instrum. Methods Phys. Res. Sect. A* 810 (2016) 1–5.
- [5] T. Kato, G. Okada, K. Fukuda, T. Yanagida, Development of BaF<sub>2</sub> transparent ceramics and evaluation of the scintillation properties, *Radiat. Meas.* 106 (2017) 140–145.
- [6] T. Murakami, J.H. Ouyang, S. Sasaki, K. Umeda, Y. Yoneyama, High-temperature tribological properties of Al<sub>2</sub>O<sub>3</sub>, Ni–20 mass% Cr and NiAl spark-plasma-sintered composites containing BaF<sub>2</sub>-CaF<sub>2</sub> phase, *Wear* 259 (2005) 626–637.
- [7] R. Tsukamoto, M. Muraoka, M. Seki, H. Tabata, I. Yamashita, Synthesis of CoPt and FePt<sub>3</sub> nanowires using the central channel of tobacco mosaic virus as a biotemplate, *Chem. Mater.* 19 (2007) 2389–2391.
- [8] J. Zhou, Z.Z. Fu, D.W. Gao, F.M. Gao, N. Li, X.N. Zhao, Y.P. Liu, Z. Wang, G.X. Wang, Fabrication of gold nanochains with octreotide acetate template, *J. Nanomater.* 2013 (5) (2013) 346274, <https://doi.org/10.1155/2013/346274>.
- [9] Z. Wu, Z.K. Wu, H. Tang, L.J. Tang, J.H. Jiang, Activity-based DNA-gold nanoparticle probe as colorimetric Biosensor for DNA methyltransferase/glycosylase assay, *Anal. Chem.* 85 (9) (2013) 4376–4383.
- [10] G.G. Pang, M.X. Sun, P. Liu, L. Hou, F.M. Gao, Facile synthesis of Pd nanostructures with enhanced electrocatalytic performance for ethanol oxidation by a bio-based method, *RSC Adv.* 6 (24) (2016) 19734–19741.
- [11] L. Han, L.P. Liu, H.J. Zhang, F. Li, A.H. Liu, Phage capsid protein-directed MnO<sub>2</sub> nano-sheets with peroxidase-like activity for spectrometric biosensing and evaluation of antioxidant behaviour, *Chem. Commun.* 53 (37) (2017) 5216–5219.
- [12] X.N. Zhao, D.W. Gao, F.M. Gao, N. Li, H. Zhou, J.K. Hao, Self-assembled platinum nanochains based on octreotide acetate, *J. Nanopart. Res.* 15 (9) (2013) 1–7.
- [13] N. Ma, E.H. Sargent, S.O. Kelley, Biotemplated nanostructures: Directed assembly of electronic and optical materials using nanoscale complementarity, *J. Mater. Chem.* 18 (9) (2008) 954–964.
- [14] Y. Liu, Y.G. Ke, H. Yan, Self-assembly of symmetric finite-size DNA nanoarrays, *J. Am. Chem. Soc.* 127 (49) (2005) 17140–17141.
- [15] N. Chelyapov, Y. Brun, M. Gopalkrishnan, D. Reishus, B. Shaw, L. Adleman, DNA triangles and self-assembled hexagonal tilings, *J. Am. Chem. Soc.* 126 (43) (2004) 13924–13925.
- [16] P.W.K. Rothmund, Folding DNA to create nanoscale shapes and patterns, *Nature* 440 (7082) (2006) 297–302.
- [17] L.L. Qian, Y. Wang, Z. Zhang, J. Zhao, D. Pan, Y. Zhang, Q. Liu, C.H. Fan, J. Hu, L. He, Analogic China map constructed by DNA, *Chin. Sci. Bull.* 51 (24) (2006) 2973–2976.
- [18] C.A. Mirkin, R.L. Letsinger, R.C. Mucic, J.J. Storhoff, A DNA-based method for rationally assembling nanoparticles into macroscopic materials, *Nature* 382 (6592) (1996) 607–609.
- [19] J.Y. Chen, X.H. Ji, Z.K. He, Smart composite reagent composed of double-stranded DNA-templated copper nanoparticle and SYBR Green I for hydrogen peroxide related biosensing, *Anal. Chem.* 89 (7) (2017) 3988–3995.
- [20] S. Pan, T.I.N.G. Li, M. Olvera de la Cruz, Molecular dynamics simulation of DNA-directed assembly of nanoparticle superlattices using patterned templates, *J. Polym. Sci. Polym. Phys.* 54 (17) (2016) 1687–1692.
- [21] C.Y. Lee, K.S. Park, Y.K. Jung, H.G. Park, A label-free fluorescent assay for deoxyribonuclease I activity based on DNA-templated silver nanocluster/graphene oxide nanocomposite, *Biosens. Bioelectron.* 93 (2017) 293–297.
- [22] E. Braun, Y. Eichen, U. Sivan, G. Ben-Yoseph, DNA-templated assembly and electrode attachment of a conducting silverwire, *Nature* 391 (1998) 775–784.
- [23] R. Seidel, L.C. Ciacchi, M. Weigel, W. Pompe, M. Mertig, Synthesis of platinum cluster chains on DNA templates: Conditions for a template-controlled cluster growth, *J. Phys. Chem. B* 108 (30) (2004) 10801–10811.
- [24] J. Richter, M. Mertig, W. Pompe, I. Mönch, H.K. Schackert, Construction of highly conductive nanowires on a DNA template, *Appl. Phys. Lett.* 78 (4) (2001) 536–538.
- [25] J. Richter, R. Seidel, R. Krisch, M. Mertig, W. Pompe, J. Plaschke, H.K. Schackert, Nanoscale palladium metallization of DNA, *Adv. Mater.* 12 (7) (2000) 507–510.
- [26] J.J. Su, F.M. Gao, L. Hou, DNA-templated assemblage of ZnS nanoparticle wires, *Nanopart. Lett.* 92 (2013) 206–209.
- [27] B. Nithyaja, K. Vishnu, S. Mathew, P. Radhakrishnan, V.P.N. Nampoori, Studies on CdS nanoparticles prepared in DNA and bovine serum albumin based biotemplates, *J. Appl. Phys.* 112 (6) (2012) 064704.
- [28] N. Li, F.M. Gao, L. Hou, The Method of Synthesis of Barium Fluoride Nanoball using DNA as Template, *China, ZL 200810079482* (2010) 9.
- [29] J.H. Cui, H.X. Cui, Y. Wang, C.J. Sun, X. Zhao, Research and application progress on using DNA as nanomaterial, *Mater. Prot.* 46 (1) (2013) 106–111.
- [30] Y.K. Gao, X.M. Zhao, P.G. Yin, Fabrication of ZnS nanocircles using Escherichia coli DNA as templates, *Mater. Lett.* 131 (2014) 112–115.
- [31] N. Li, F.M. Gao, L. Hou, D.W. Gao, DNA-templated rational assembly of BaWO<sub>4</sub> nano pair-linear arrays, *J. Phys. Chem. C* 114 (2010) 16114–16121.
- [32] R. Nambiar, B. Sonday, J.C. Meiners, Thermal fluctuations of extended DNA single molecules, *Int. Soc. Opt. Eng.* 5841 (2005) 103–109.